Simultaneous Photoelectron and Ion Measurements in the Martian Tail

R. A. Frahm, J. D. Winningham, J. R. Sharber (*Southwest Research Institute, 6220 Culebra Road, San Antonio, Texas 78228, United States*), R. Lundin, H. Nilsson, S. Barabash (*Swedish Institute of Space Physics, Box 812, Kiruna S-981 28, Sweden*)
A. J. Coates, D.R. Linder (*Mullard Space Science Laboratory, University College London, Holmbury St. Mary, Dorking Rh5 6NT, United Kingdom*), A. Fedorov, and J. -A. Sauvaud (*Centre d' Etude Spatiale des Tayonnements, 9 Avenue de Colonel Roche, Toulouse 31028, France*)

Abstract

The Analyzer of Space Plasmas and Energetic Atoms (ASPERA-3) experiment on board the Mars Express (MEx) spacecraft conducts of measurements of electrons by the Electron Spectrometer (ELS), ions by the Ion Mass Analyzer (IMA), and neutral particles by the Neutral Particle Imager (NPI) and the Neutral Particle Detector (NPD). While orbiting Mars, the ELS is able to observe peaks in the photoelectron spectrum due to photoionization of carbon dioxide and atomic oxygen by Solar Helium 30.4 nm photons. The source of these peaks is the dayside Martian ionosphere, with the majority of photoelectrons created at the exobase where the density is greatest. A fraction of these photoelectrons is transported to altitudes of the spacecraft. By the time the atmospheric photoelectrons reach the spacecraft in the tail of Mars, their pitch angles have narrowed. Changes in the orientation of the ASPERA-3 experiment has reduced the amount of the atmospheric photoelectron distribution which is observed. However, recent improvements in the sensitivity of IMA have made possible the detection of low-energy ions at the same time as photoelectrons in the ionosphere. Fluxes of both ions and electrons are observed to decrease with increasing distance away from the planet. Due to the current operation of ASPERA-3, the measurement planes of ELS and IMA are not co-planar causing photoelectron peaks and low-energy ions to be observed at different times and in different directions making coincidence arguments difficult.

Introduction

Since December 25, 2003, the Mars Express (MEx) spacecraft has been orbiting Mars. MEx measurements of the Martian particle environment have been performed by the Analyzer of Space Plasmas and Energetic Atoms (ASPERA-3) Experiment [Barabash *et al.*, 2004], which measures electrons with the Electron Spectrometer (ELS), ions with the Ion Mass Analyzer (IMA), and neutral particles with the Neutral Particle Detector (NPD) and Neutral Particle Imager (NPI). Since arriving at Mars, ELS has measured peaks in the photoelectron spectrum [Coates *et al.*, 2004; Frahm *et al.*, 2004]. These photoelectron peaks are attributed to both carbon dioxide and atomic oxygen, and are theoretically located in energy between 21 eV and 24 eV, and 27 eV [Mantas and Hanson, 1979].

The ELS observation of photoelectron peaks in the energy spectrum are mainly due to ionization of carbon dioxide with Solar 30.4 nm photons near the Martian exobase, and transported to higher altitudes [Mantas and Hanson, 1979; Fox and Dalgarno, 1979]. Near the Martian exobase, the concentration of carbon dioxide is about 50 times greater than atomic oxygen, which is also known to be ionized by Solar 30.4 nm photons and produce peaks in the electron spectrum near those of carbon dioxide. The energy resolution of ELS (about 8%) is too large to distinguish between the energy spectrum of electrons photoionized from carbon dioxide and those from atomic oxygen. At altitudes above about 210 km, atomic oxygen becomes the dominate species over carbon dioxide (down by about a factor of 1000 from its peak production rate). Locally produced electrons from ionization (at spacecraft altitudes) of the atomic oxygen occur more frequently then by locally produced electrons from ionization of carbon dioxide. ELS can not distinguish between photoelectrons produced locally and those transported to the sensor. Thus, ELS measurements of electrons in the region of the photoelectron peaks may be produced by both carbon dioxide and atomic oxygen, and generated both locally or transported to the instrument.

After the carbon dioxide or atomic oxygen are ionized, the charged components are subject to the local magnetic field and are transported accordingly [Mantas and Hanson, 1979]. The ASPERA-3 ELS has observed photoelectron peaks in the Martian induced magnetosphere while orbiting the planet at various altitudes [Frahm et al, 2006a,b]. During the nominal mission of Mars Express, the IMA sensitivity was tuned to measure escaping higher-energy ions and the capability to observe low-energy ions was limited. Late in the spring of 2007 the IMA was reprogrammed to increase its sensitivity to lower-energy ions. This resulted in the detection of low-energy planetary ions in the Martian ionosphere which were components of carbon dioxide. Ions in the Martian ionosphere are observed to be directional; however, because of their low-energy being near the IMA energy threshold, detection may be a result of ion flow caused by the ram pressure of the spacecraft motion combined with spacecraft potential [Frahm *et al.*, 2007] (i.e., not a real flow).

Electron Tail Observations

Many observations of photoelectron peaks in the tail of Mars have shown that the peaks are strong features which dominate the electron spectrum. Photoelectron peaks in the tail are readily identifiable and consistent. Examples of photoelectrons in the tail of Mars are shown on 15 July 2007. Figure 1 shows the MEx spacecraft orbit around Mars in cylindrical coordinates with the location of the spacecraft marked every 10 minutes. Highlighted are locations where photoelectron peaks are observed. During this transit, photoelectron peaks are observed by different sectors of the ELS at different times. Highlighted areas are marked with the ELS sector exhibiting the strongest photoelectron peak signal using the format ELS-xx, where xx is the sector number. ELS sectors measure 22.5° around a 360° entrance plane, numbered 00 through 15 to designate each sector's look direction.

MEX position every 10 min. Cylindric coordinates. Orbit 4530
Pericenter at 2007-0715 03:16:03 Start at 2007-07-14 23:54;27 End at 2007-07-06:37:37

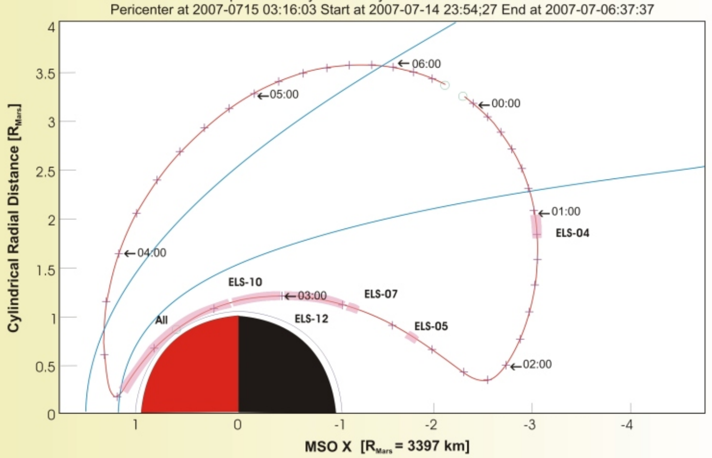

Figure 1. The Orbit of the Mars Express Spacecraft on 15 July 2007. The spacecraft orbit is shown in a cylindrical Mars-centered Solar Orbital (MSO) coordinate system with the Sun at the left. Sketched in blue are the average locations of the bow shock, magnetic pile-up boundary, and photoelectron boundary as determined using Mars Global Surveyor data [Vignes *et al.*, 2000]. The location of the spacecraft is marked in UT every 10 minutes and labeled every hour. Locations where the photoelectron peaks are observed are highlighted. When the photoelectron peaks are prominent within an ELS sector, this is noted near the corresponding highlighted region.

Figure 2 shows the energy-time spectrograms for each ELS sector between about 3000 km altitude and periapsis in units of differential energy flux, with the color scale adjusted to highlight the peaks in the photoelectrons. Fluxes in the dayside ionosphere are observed when the Solar Zenith Angle (SZA) is less than 90°. A comparison of the photoelectron peaks which are observed by various sectors illustrate that outside the ionosphere, the peaks only appear in selected sectors and not in all sectors as they do in the dayside ionosphere. For the case of this pass, the scanner is parked with a 10° offset, which places sectors 0, 13, 14, and 15 viewing toward the spacecraft body and sector 12 partially viewing over the spacecraft.

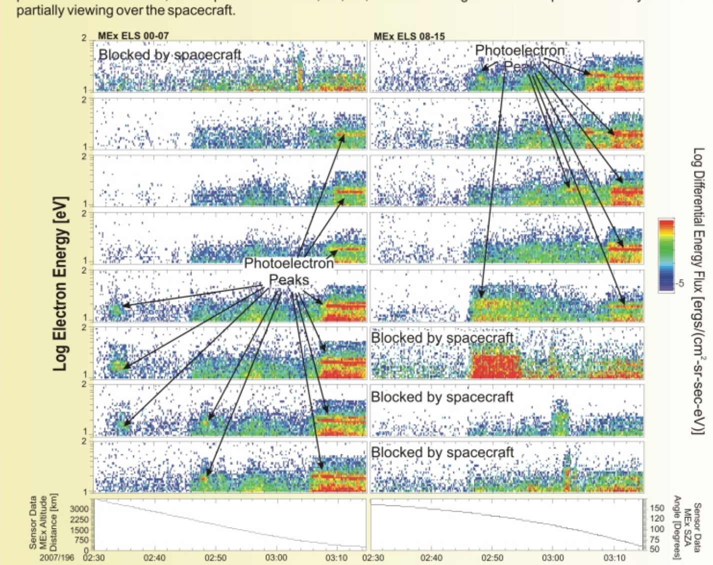

Figure 2. Energy-Time Spectrogram of Electrons Measured on 15 July 2007 from an Altitude of 3000 km to Periapsis. Shown are spectrograms from the 16 ELS sectors (first 8 on the left, second 8 on the right, numbered lowest at top to highest at bottom) above drawings of the spacecraft altitude (left) and solar zenith angle (right). The color scale for the differential energy flux values has been adjusted to emphasize observations of photoelectron peaks.

In order to further illustrate the flux spectrum, we show four examples of the electron spectrum in Figure 3. In Figure 3a, we show the differential number flux of electrons from ELS-05 averaged between 02:32:32 UT and 02:34:46 UT (about 3000 km altitude in the tail) and 03:13:59 UT to 03:16:14 UT (near dayside periapsis). The overall spectrum at 3000 km is not as intense as the periapsis spectrum, which is a common feature observed: in general, the further away from the planet, the less intense the spectrum. However, in both cases, the photoelectron peaks are observed easily. It should be noted that the photoelectron peaks are shifted from their theoretical value and at periapsis (3000 km) the inferred spacecraft potential is about -4 volts (-8 volts).

The photoelectron peak is a strong feature at times, but it is not as strong at other times. Figure 3b illustrates the differential number flux of electrons from ELS-04 averaged between 01:03:30 UT and 01:08:06 UT (about 8900 km altitude in the tail) and 03:13:59 UT to 03:16:14 UT (near dayside periapsis). These photoelectron peaks are shifted from their theoretical value such that at 9800 km, the inferred spacecraft potential is about -14 volts. Due to the sampling of ELS, there are other times when the highest energy photoelectron peak is not prominent. Figure 3c illustrates the differential number flux of electrons from ELS-07 averaged between 02:47:28 UT and 02:49:43 UT (about 2100 km altitude in the tail) and 03:13:59 UT to 03:16:14 UT (near dayside periapsis). These photoelectron peaks are shifted from their theoretical value such that at 2100 km, the inferred spacecraft potential is about -5 volts. Both effects can combine at times to make identification difficult. In addition, the spacecraft can interact with electrons in the peak, blurring their structure as in Figure 3d. Figure 3d illustrates the differential number flux of electrons from ELS-12 averaged between 02:50:29 UT and 02:52:44 UT (about 1800 km altitude in the tail) and 03:13:59 UT to 03:16:14 UT (near dayside periapsis). These photoelectron peaks are shifted from their theoretical value such that at 1800 km, the inferred spacecraft potential is about -1 volt. Here it should be noted that since the distinct peak structure is not discernible, spacecraft potential is more difficult to determine.

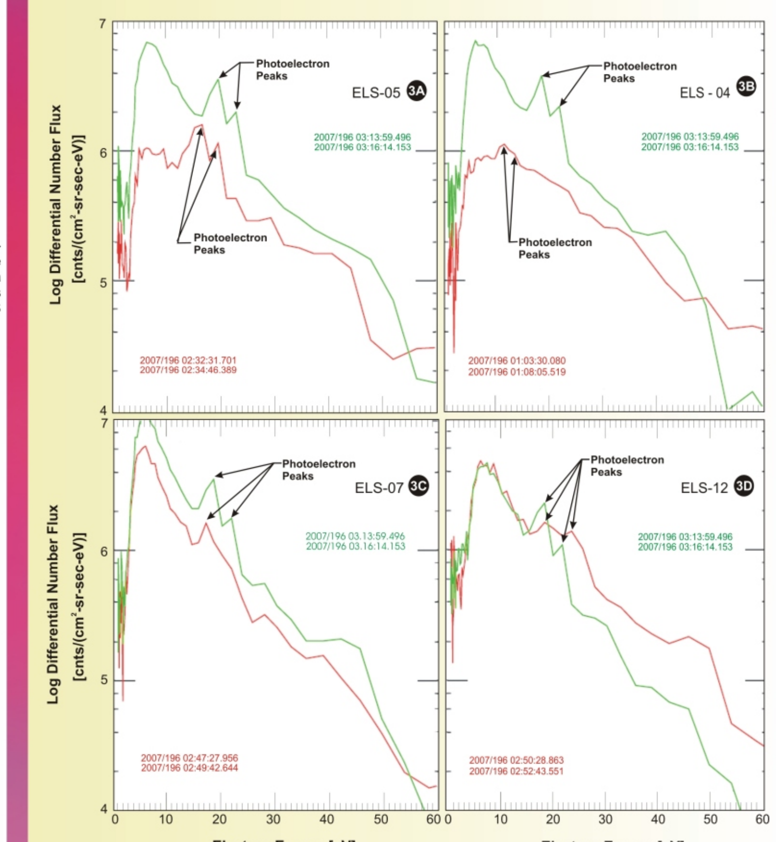

Figure 3. Selected Electron Energy Spectra. Four types of differential number flux spectra containing photoelectron peaks are presented. Each type is shown in red during tail measurements and green when measurements are in the dayside ionosphere. Spectrum a) occurs in ELS-05 and shows two peaks similar to the dayside ionosphere, b) occurs in ELS-04 and shows lower amplitude peaks in the tail, c) occurs in ELS-07 and shows only one photoelectron peak, and d) shows flux from ELS-12 influenced by the spacecraft.

Ion Tail Observations

Low-energy planetary ions are often observed in the Martian tail. For the same time period as the electrons shown by Figure 2, the ion energy-time spectrogram shown in Figure 4 is displayed in differential energy flux using a color range and energy scale appropriate to highlight the low-energy ions. Similar to the angular behavior of the electrons, the low-energy ion flux is highly directional, both in the tail and in the ionosphere. Ion fluxes between 0230 UT and 0256 UT are strongest in IMA-00, whereas in the ionosphere (after 0310 UT), fluxes are strongest in IMA-13. Between 0300 UT and 0307 UT, there are weak fluxes of low-energy ions observed in IMA-00.

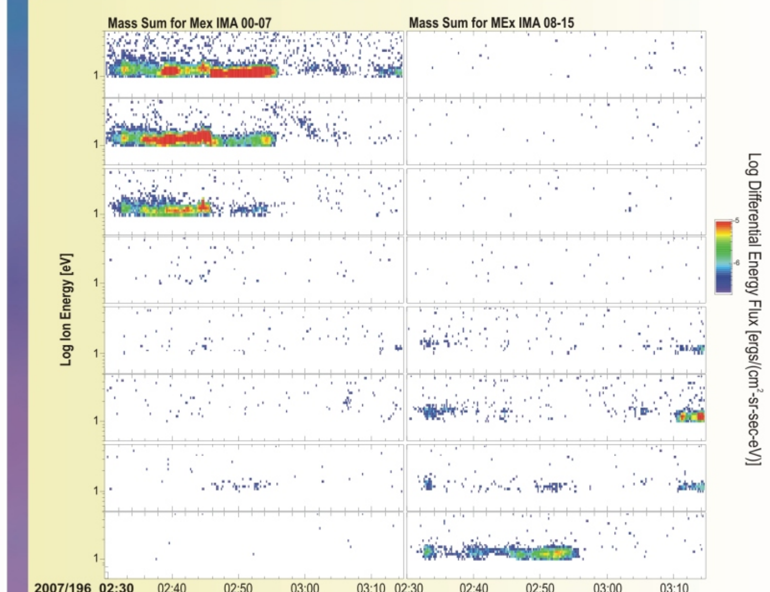

Figure 4. Energy-Time Spectrogram of Ions Measured on 15 July 2007 from an Altitude of 3000 km to Periapsis. Shown are spectrograms from the 16 IMA sectors (first 8 on the left, second 8 on the right, numbered lowest at top to highest at bottom). The low-energy range detected by IMA and the color of the differential energy flux values has been adjusted to emphasize observations of low-energy ions.

The ion mass spectra corresponding to the selected electron spectra from Figure 3 are shown in Figure 5. In all cases, the vertical scale shows the ion energy between 5 eV and 50 eV, and the horizontal scale is expressed in terms of mass channel number. The mass channel number location of a species is dependent on the ion energy and instrument settings. For these measurements, the locations of where various mass species are recorded are indicated in each spectrum as overlaid lines with the species marked. All spectra are shown in units of differential energy flux. Figure 5a shows the ion mass spectrum from IMA-00 averaged between 02:32:23 UT and 02:34:47 UT, and represents the ions detected in the range of 3000 km altitude in the Martian tail. Here the IMA shows masses in the region where ionization products of carbon dioxide (including ionized atomic oxygen) are expected. Deeper in the tail (about 8900 km altitude) the IMA the ion mass spectrum from IMA-00 averaged between 01:03:23 UT and 01:08:11 UT (Figure 5b) resembles only noise and no detectable mass is observed. The effect of spacecraft charge of -14V should have accelerated low-energy ions into the energy range detectable by IMA if they were present; however, electron fluxes were lowest for this spectrum and it is very possible that the measurement threshold for flux in IMA is not enough to detect ions in this case, so this fact should be acknowledged requiring that fluxes at large tail distances be further examined.

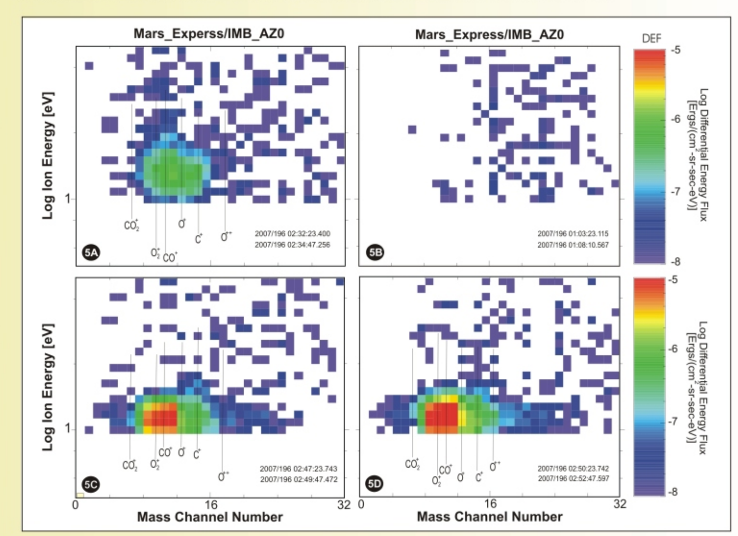

Figure 5. Selected Ion Energy Spectra. Four time periods of differential energy flux spectra containing low-energy for IMA-00 are presented. Locations of various species (ionization products of carbon dioxide) are drawn on top of ion mass channel spectra. Spectrum a) occurs during the time ELS-05 shows two photoelectron peaks, b) occurs during the time ELS-04 shows lower amplitude photoelectron peaks in the Martian tail, c) occurs during the time ELS-07 shows only one photoelectron peak, and d) occurs during the time ELS-12 shows influence by the spacecraft.

The ion spectra for the third case of a single photoelectron peak is shown in Fingure 5c, averaged from 02:47:24 UT to 02:49:47 UT. Here the IMA also shows ionization products of carbon dioxide (including ionized atomic oxgyen) and the flux level at about 2100 km altitude is greater than that of the flux measurement at 3000 km by about an order of magnitude. Decreasing the altitude a bit continues to increase the flux of ions as shown in Figure 5d averaged from 02:50:24 UT to 02:52:48 UT in the range of 1900 km altitude. Again, Ionization products of carbon dioxide are observed.

The increase of flux with decreasing altitude does not continue through to periapsis for this case. Since periapsis ion fluxes were greatest in IMA-13, the ion mass spectra for IMA-13 averaged from 03:13:60 UT to 03:16:24 UT are shown in Figure 6. The ion mass spectra shows that ionization products of carbon dioxide are observed and are in similar ratios to fluxes presented at 1900 km and 2100 km altitudes.

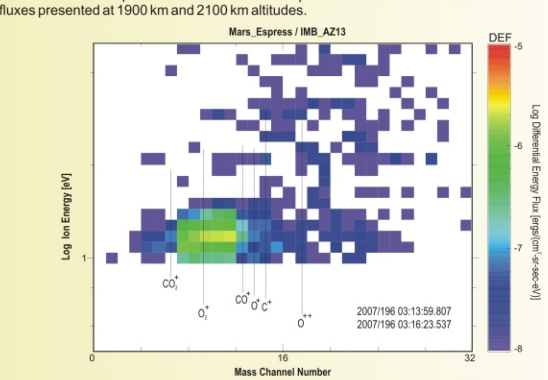

Figure 6. Periapsis Ion Energy Spectra. Spectra shown in the ionosphere do not exhibit differential energy fluxes with as high an amplitude as those of Figure 5d.

Discussion

ELS exhibits photoelectron peaks from the ionization of carbon dioxide and atomic oxygen, which in the Martian tail are directional. During times when these photoelectron peaks are observed, there exist low-energy ions.These low-energy ions are also directional in the Martian tail, but unlike the electrons which are mostly isotropic in the Martian ionosphere, ions in the ionosphere are anisotropic (as shown here and in Frahm *et al.*, 2007). On this pass, a rough correlation exists between the intensity of the differential energy flux of ions and the distance from the planet in the tail (Figure 5). Tail fluxes were shown to be more intense than those of the ionosphere. Frahm *et al.* [2007] showed an example of ion differential energy flux in the Martian ionosphere which was as intense as the fluxes shown in Figure 5d. During the measurements on 15 July 2007, IMA was not scanning in elevation. It is likely that the peak of the ion flux within the ionosphere was not within IMA's measurement plane.

Prior to the movement of the ASPERA-3 scanner in early 2006, the ELS and central IMA measurement planes were co-planar. However, the ASPERA-3 scanner is now used for minor scanning and positioning its electron and neutral imager sensors so that the Sun does not shine in the apertures of the neutral imaging instruments. This results in the the measurement planes of ELS and IMA not being co-planar most of the time data is acquired. Thus, the IMA and ELS often do not view plasma flow in the same or a similar direction. During the data collection period presented here, the ELS measurement plane is tilted about 80° from the IMA measurement plane, with two intersection locations, the first being in the ELS-00 and ELS-15 sectors measuring about in the same direction as IMA-04 and IMA-05, and the second being in the ELS-07 and ELS-08 sectors measuring about in the same direction as IMA-12 and IMA-13. For reference, the ELS-04 and IMA-00 are viewing in the same direction if co-planer, but here they are separated by about 80°.

When surveying electron and ion spectra, times have been observed where there are low-energy ions but no photoelectron peaks and other times where there are photoelectron peaks but no low-energy ions. It is difficult to assess whether or not the low-energy ions are co-located with the photoelectrons which come from the dayside atmosphere of Mars because the ELS and IMA are not observing plasma in the same plane. Further data where ELS and IMA observe in the same plane are needed to address this issue.

These results presented here are (or may be) consistent with the escape mechanism suggested by Coates *at al.* [2007], that excaping photoeletrons at Titan set-up ambipolar electric field which pull ions out from the planetary ionosphere to form a polar wind. It is possible that a similar escape mechanism exists at Mars.

Conclusion

On a representative pass through the Martian tail region, *in situ* instruments of the ASPERA-3 experiment on Mars Express have measured low-energy ions concurrently with ionospheric photoelectron peaks. The photoelectron peaks can be observed as a single peak or multiple peaks due to the instrument response function of ELS and the energy of the peak as modified by the potential on the spacecraft. In cases where electrons from the photoelectron peaks encounter the spacecraft before detection, they can react with the spacecraft sheath and distort the electron energy spectrum.

Low-energy ions can also be observed when photoelectron peaks are observed. However, viewing geometry is not ideal and this leads to an ambiguity between the flow direction of low-energy ions and electrons in the photoelectron peaks. Under most circumstances, both the low-energy ions and electrons in the photoelectron peaks lose intensity as they travel down tail. Low-energy ions are comprised of cold planetary ions from the ionized components of carbon dioxide (CO_2^+, O_2^+, CO^+, C^+, and O^+).

References

Barabash, S., *et al.*, "ASPERA-3: Analyser of Space Plasmas and Energetic Ions for the Mars Express," in Mars Express: The Scientific Payload, eds., A. Wilson and A. Chicarro, European Space Agency special report SP-1240, European Space Agency Research and Scientific Support, European Space Research and Technology Centre, Noordwijk, The Netherlands, 121-139, August 2004.
Coates, A. J., *et al.*, "Electron observations from Mars Express ASPERA-ELS," presented at International Mars Conference, Ischia, Italy, 19-23 September 2004.
Coates, A. J., *et al.*, "Ionospheric electrons in Titan's tail: plasma structure during the Cassini T9 encounter," Geophys. Res. Lett., 34, L24S05 oi:10.1029/2007GL030919, October 18, 2007.
Fox, J. L., and A. Dalgarno, "Ionization, Luminosity, and Heating of the Upper Atmosphere of Mars," Journal of Geophysical Research, 84, 7315-7333, 1979.
Frahm, R. A., *et al.*, "First Observations from the ASPERA-3 ELS in the Mars Ionosphere," EOS Transactions of the American Geophysical Union, 85(17),Joint Assembly Supplement JA353, Abstract SA32B-02, May 18, 2004.
Frahm, R. A., *et al.*, "Carbon dioxide photoelectron energy peaks at Mars," Icarus, 182, 371-382, 2006a.
Frahm, R. A., *et al.*, "Locations of Atmospheric Photoelectron Energy Peaks within the Mars Environment," Space Science Reviews, 126(1-4), 389-402, 2006b.
Frahm, R. A., *et al.*, "Simultaneous Photoelectron and Ion Measurements in the Martian Ionosphere," presented at the European Mars Science and Exploration Conference: Mars Express & ExoMars, European Space Research and Technology Centre (ESTEC), Noordwijk, The Netherlands, November 15, 2007.
Lundin, R., *et al.*, Solar Wind-Induced Atmospheric Erosion at Mars: First Results from ASPERA-3 on Mars Express," Science, 305, 1933-1936, 2004.
Mantas, G. P., and W. B. Hanson, "Photoelectron Fluxes in the Martian Ionosphere," Journal of Geophysical Research, 84, 369-385, 1979.
Vignes, D., *et al.*, "The Solar Wind Interaction with Mars: Locations and Shapes of the Bow Shock and the Magnetic Pile-up Boundary from Observations of the MGS/ER Experiment on Board Mars Global Surveyor," Geophysical Research Letters, 27(1), 49-52, 2000.